Experimental assessment of the RESCUE collision mitigation system

R. Labayrade, C. Royere, D. Aubert

IEEE Transactions on Vehicular Technology, Vol 56 Issue:1, Jan. 2007, pp 89 - 102
DOI: 10.1109/TVT.2006.883780

Sponsored by: IEEE Vehicular Technology Society
http://ieeexplore.ieee.org/xpl/RecentIssue.jsp?punumber=25

Experimental Assessment of the RESCUE Collision Mitigation System

Raphael Labayrade[1], Cyril Royere[2] and Didier Aubert[3]

LIVIC - INRETS / LCPC

14, route de la Miniere

Batiment 824

78000 Versailles

France

[1]: e-mail: raphael.labayrade@lcpc.fr, tel: +33 1 40 43 29 32

[2]: e-mail: cyril.royere@inrets.fr, tel: +33 1 40 43 29 14

[3]: e-mail: didier.aubert@inrets.fr, tel: +33 1 40 43 29 18

Abstract

Road traffic incidents analysis has shown that 52% of them are caused by a collision between two vehicles or between a vehicle and an obstacle. In this paper, the RESCUE (that stands for REduce Speed of Collision Under Emergency) collision mitigation system (version 1.0) is presented and evaluated towards various typical road situations. The aim of the RESCUE system is to decrease the kinetic energy dissipated during a collision through automatic emergency braking that occurs 1 second before the collision. This emergency braking is triggered by an alarm coming from a decision unit taking into consideration the results of a generic obstacles detection system -based on fusion between stereovision and laser scanner- and a warning area in front of the vehicle. The different sub-systems are presented. Then, the behavior of the RESCUE collision mitigation system towards various typical dangerous road situations is assessed through systematic tests. These quantitative tests are completed by qualitative ones carried out on 737 *km* of open roads (freeways, highways, rural roads, downtown) so as to provide a more precise idea about the false alarm rate. The experiments show the system is promising in terms of reliability, genericity and efficiency.

Keywords: Collision Mitigation, Experimental Assessment, Sensors Fusion.

I. INTRODUCTION

In Europe, more than 52% of road accidents are caused by a collision between two vehicles or between a vehicle and an obstacle [1]. Moreover, research has shown that $90\% - 95\%$ of road accidents are partly caused by human errors [2]. For instance, before a collision, many drivers do not activate a braking pressure appropriate to the situation or completely release the brake: 39% of the drivers do not brake at all. Thus, in the context of active safety and Advanced Driving Assistance Systems, a collision mitigation system aiming at reducing the kinetic energy dissipated during a collision or stopping the vehicle before the collision -if its velocity is low- could decrease the number and the damage of road accidents. Moreover, 74% of the total number of accidents occur in the urban area. Consequently, a collision mitigation system should be efficient not only on freeways or highways but also in urban and downtown areas.

Collision mitigation systems have been subject to investigation for several years [3][4][5]. In the framework of the PREDIT[1] French program in the context of the ARCOS[2] project [6], a system called RESCUE (that stands for REduce Speed of Collision Under Emergency) has been developed. It was designed taking into consideration it had to be efficient in any kind of road situations, including urban areas. This requires the system to be very reactive in order to handle obstacles appearing suddenly (such as pedestrians) and typical urban situations such as crossroads. In the early stages of development, various operating modes were introduced for this system.

The less intrusive mode is the *instrumented mode*, that only informs the driver of the distance and Time To Collision (TTC) of the nearest obstacle. Clearly, the risk of collision increases when the TTC decreases. Thus, in order to avoid any risk of collision, the driver should keep the TTC above 2 seconds, for instance.
In order to assist the driver, more advanced modes have been developed. All are based on a risk indicator, computed from the measured TTC -the risk becomes higher when the TTC of the nearest obstacle decreases.
Thus, the *warning mode* sends a warning (for example acoustic or haptic warning) to the driver when the risk indicator is above a first threshold. This mode is intended to alert the driver in advance for starting a manoeuver -for example, a braking manoeuver; the warning lights should also be turned on to warn the surrounding vehicles.
The next mode, the so-called *limit mode* is the first active mode: it prevents the risk indicator to become too high, through the use of activators in the vehicle. Thus, in the case of the RESCUE system, the *limit mode* launches an automatic braking when the TTC of the nearest obstacle drops under a second threshold.
The most intrusive mode is the *regulated mode* that keeps the risk indicator at a constant level, through the use of activators -the throttle and the brake. In other words, the *regulated mode* can be seen as a full automated mode, that keeps the TTC at a value of 2 seconds, for instance.
The first three modes (*instrumented, warning* and *limit*) have been implemented in a prototype vehicle. Yet, a collision mitigation system is usually described as a last resort system, aimed at launching an automatic emergency

[1]National Transport Research Program

[2]Research Action for Secure Driving

braking to reduce the kinetic energy of a collision. Thus, the operating mode that best corresponds to this definition is the *limit mode* we focus on in this paper.

A crucial point for the efficiency and the acceptability of driving assistance systems is the adjustment of the launch thresholds. Thus, the emergency braking should intervene in situations where the driver has physically no chance to avoid a collision by himself. Assessing wether a driver has such a chance is a difficult task depending on the driver state, experience and behavior and on the road and driving contexts. In this paper, we assume the driver is a common driver whose average reaction time is about 1 second, and we consider that he has no chance to avoid a collision by himself if he has not reacted when the TTC is below its average reaction time. Thus, we consider that the emergency braking should be launched when the TTC of the nearest obstacle drops under 1 second.

In order to be efficient on any road, including urban roads, the system must be reactive and must handle situations where the road is narrow or presents tight curves or longitudinal curvature. It must also be able to cope with a large number of obstacles at the same time.
Thus, the system we focus on in this paper is made of three sub-systems designed to meet these requirements. The first one is a generic obstacles detection system designed to be reactive and to cope with all types of road geometry, including non planar surfaces. The second one is a warning area generator, aimed at predicting the path of the equipped vehicle in order to avoid taking into consideration obstacles that will not collide it, and to handle narrow roads and tight curves. The third sub-system is the very automatic braking system which is used to dissipate the kinetic energy of the vehicle before a collision.

Concerning the first sub-system, it is clear in literature that obstacles detection has been subject to many investigation for years. Sensors like vision [7], laser scanner [8] or radar [9] are usually used to this purpose. In order to obtain a reliable, reactive and accurate system, performing data fusion between various sensors is also proposed frequently for the development of Advance Driver Assistance Systems [4][5][10][11][12][13]. For instance, using two complementary sensors such as stereovision and laser scanner can be an efficient solution [14]. Indeed laser scanner is accurate and fast, but this sensor cannot be used alone because of false alarms occurring when the laser points collide with the road surface (because of road geometry and vehicle pitching). On the other hand, stereovision allows to model the road geometry and extract obstacles in a robust manner [15]; yet it is not accurate enough to compute precise velocities and TTC (because of the size of the back-projected area in the road scene corresponding to a pixel in the image). However accuracy of the TTCs estimation is a crucial point in any collision mitigation system. Thus, a fusion strategy between these two sensors is proposed in this paper.
Concerning the warning area generator, a process using some vehicle ego parameters is proposed.
Eventually, to be as efficient as possible, the automatic braking system is based on an additional brake circuit.
These three subsystems are detailed in section II.

In order to assess the efficiency and the safety of the RESCUE system, quantitative and qualitative experiments have been carried out. In section III, various typical scenarios (mainly urban scenarios) are introduced and systematic

tests are carried out: 16 scenarios are introduced, and 10 tests are carried out for each one. Additional tests in countryside, highways, freeways and downtown are also presented to provide a more precise idea about the false alarm rate in real driving situations.
We discuss the remaining issues and give some ideas to tackle them in section IV.

II. THE RESCUE COLLISION MITIGATION SYSTEM

The RESCUE collision mitigation system can be divided into three sub-systems and a decision unit that interconnects these sub-systems. An overview of the whole system is presented on Figure 1. The first sub-system is a generic obstacles detection system, performing data fusion between stereovision and laser scanner.
The second sub-system is the so-called warning area generation system that uses an odometer and an inertial sensor. The decision unit checks wether an obstacle is located in the warning area, and wether its TTC is under 1 second; if so, a warning message is sent to the third sub-system.
The third sub-system is the automatic braking system, based on an additional brake circuit activated when a warning message is received.

[Figure 1 about here.]

[Figure 2 about here.]

A. Obstacles detection system

The obstacles detection system is based on fusion between stereovision and laser scanner. This system began to be designed in [14]. We give here an overview of the algorithm and propose improvements. A synoptic of the algorithm is presented on Figure 2.

1) Stereovision based detection: The stereovision algorithm uses the "v-disparity" transform to perform robust and generic obstacles detection [15].

This algorithm assumes the road scene is composed of set of planes: obstacles are modelized as vertical planes, whereas the road is supposed to be an horizontal plane (when it is planar), or a set of oblique planes (when it is not planar). The algorithm performs a robust extraction of these planes from which it deduces many useful information about the obstacles located on the road: for instance, their distances, lateral positions, contact lines with the road, bounding boxes. Figure 3 illustrates the outline of the process. From the two stereo images (a) and (b), a disparity map I_Δ (c) is computed (Sum of Square Differences -SSD- criteria is used to this purpose along edges). The disparity values are represented by a grey level according to the corresponding scale given on the left. Then an accumulative projection of this disparity map is performed to build the "v-disparity" image $I_{v\Delta}$ (d). For the image line i, the abscissa u_M of a point M in $I_{v\Delta}$ corresponds to the disparity Δ_M and its grey level i_M to the number of points with the same disparity Δ_M on the line i : $i_M = \sum_{P \in I_\Delta} \delta_{v_P,i} \delta_{\Delta_P,\Delta_M}$ where $\delta_{i,j}$ denotes the Kronecker delta. From this "v-disparity" image, a robust extraction of straight lines is performed through a Hough transform

(e). This extraction of straight lines (f) is equivalent to the extraction of the planes of interest taken into account in the modelization of the road scene. Simple geometric considerations allow to deduce the useful features needed for the next stages of the obstacles detection process (g) : distances to obstacles, lateral position, width.
Experimental evaluations of this algorithm has shown it is suitable for the road obstacles detection task since it is fast, generic, robust to adverse illumination and meteorological conditions [16].

[Figure 3 about here.]

2) Laser scanner based detection: Concerning the laser scanner raw processing, an autonomous clustering is performed from the laser points using Mahalanobis-like distance. An ellipsoid is build around each set of clustered laser points and is characterized by its gravity center, its orientation and the length of its two axis. Each ellipsoid is then considered as a target. The width of the target is computed as the distance along the X-axis between the two extreme laser points belonging to it. More details about this autonomous clustering can be found in [14]. Figure 4 gives an example of result of this process.

[Figure 4 about here.]

3) Tracking and association over time: The next stage of the algorithm consists in performing tracking of the detected targets for each sensor over time. A first order Kalman filtering is used to generate tracks from targets and to predict their state (position, width and orientation if available) at the next step of time. The remaining problem is to perform association between the set of targets and the set of existing tracks. This task must also manage the appearance of new targets, the periods of disappearance of tracks, and the re-association of targets with tracks (when targets have disappeared during a short time). The matching between the set of existing tracks and the set of perceived objects is performed using cartesian distance, width and orientation as chief criteria.

More precisely, the behavior of the tracking and association task is as follows :

- a target is matched to a track if both overlap. The potential overlap is checked thanks to the width and position of both track and target. If available (for the laser scanner), the matching is confirmed if the orientation of the target and of the track are close to each other, either no matching is performed,
- if a target can not be matched with any existing track, a new track is created at the position of the target,
- if a track has not been matched for 3 steps of time, it is destroyed.

This association task is performed through an algorithm implementing belief theory introduced by Dempster and Shafer [17]. This algorithm is designed to avoid the high computational cost usually observed. For more details, see [18]. Figure 5 gives an example of result of tracking of multi-objects over time. The objects are located on the X-Y plane. The vertical axis on the figure represents time. The successive positions of the objects are represented as little circles and the grey levels of these circles indicate the tracks the objects are associated to. On this figure, the appearance, disappearance and re-association stages can be observed.

[Figure 5 about here.]

In the former versions of the obstacles detection algorithm [14], tracking was performed in the "top-view" coordinate system (O, X, Y) shown on Figure 7 for targets coming from both laser scanner and stereovision sensors. This method presented some drawbacks concerning targets detected by stereovision, because the stereovision process is not accurate enough. Indeed, the back-projection from the image coordinate system to the "top-view" coordinate system is inaccurate, all the more when the targets detected by stereovision get further. This is due to the size of the back-projected area in the "top view" coordinate system corresponding to the size of a pixel. As a matter of fact, the tracking process could hardly manage far targets and provided uncorrect estimations of relative velocities used in the Kalman filtering.
In the current implementation of the algorithm, the crucial difference consists in performing the tracking process directly in the image coordinate system, and performing back-projection after the tracking process. This method proves to be more efficient and stable.

4) Fusion and certainty about the existence of an object: Since the frequencies of the laser scanner (about 38 *Hz*) and of the stereovision sensor (about 25 *Hz*) are not the same, temporal alignment must be performed before the fusion task. A first order Kalman filtering is used to predict the position and width of the tracks from both sensor at the next same step of time.
Once this temporal alignment is performed, the next task consists in checking wether a track created from the stereovision process and a track created from the laser scanner process overlap. This is done thanks to the position and width of the tracks from both sensors in the "top-view" (O, X, Y) coordinate system.

A confidence value about the existence (the so-called *certainty*) of the track is computed as follows:

- the certainty is initially set to 0,
- if an overlap is detected, the certainty is increased by an increment I_1 set to 0.3 in the system,
- if no overlap is detected, the certainty is decreased by a decrement D_1 set to 0.1 in the system,
- the certainty is limited between 0 and 1.

A track is $confirmed$ (e.g. taken into account) when its certainty is above a threshold S_0 set to 0.7 in the system. The values of I_1, D_1 and S_0 have been chosen experimentally, taking into account that a track must be confirmed quickly after its first detection, and that disappearance of short duration should not affect the behavior of the system. With the chosen values, a track is confirmed after 3 consecutive observations and the system can handle disappearances lasting up to 3 times duration of the step of time (in the prototype system the step of time lasts for 26 ms).

The final position, width, and relative velocity of a track are the ones coming from the laser scanner process which are more accurate than the corresponding values coming from the stereovision process. Thus, the stereovision is used to increase the certainty about the existence of the tracks.

5) Relative Velocity and TTC estimation: A Kalman filtering is used to estimate the relative velocity of an object with respect to the vehicle. A crucial point for fast convergence consists in making a suitable choice for the initial value of the estimated relative velocity. For non-moving obstacles, the best initial value would be the ego speed of the equipped vehicle. However the collision mitigation system must be able to cope with moving objects, including followed vehicles, whose relative velocity can be positive or negative. In this case, if the initial value of the relative speed is set to the ego speed of the vehicle, the convergence time can be too long (about 300 *ms*) to ensure the system to be reactive enough to cope with some urban situations (see in section III scenarios 5,6,7). That is why we have chosen to set the initial value of the estimated relative speed to 0 *m / s*.
Figure 6 compares the estimated relative velocity versus the velocity of the equipped vehicle given by odometer, for a motionless obstacle. The two curves are closed to each other and one can notice a $115\ ms$ time of convergence before the difference between the two velocities becomes less than 5%.

The TTC of a track is estimated as TTC = $\frac{D}{V_r}$ where D is the distance between the track and the equipped vehicle and V_r is the relative velocity of the track with respect to the equipped vehicle.

[Figure 6 about here.]

B. Warning area generation

[Figure 7 about here.]

In order to remove tracks that are not on the path of the vehicle and handle narrow roads and tight turns, we generate a *warning area* which corresponds to the prediction of the path of the vehicle in the next second (see Figure 7). To this purpose, we use the velocity V of the vehicle computed from the odometer signal and the yaw rate ψ output from the inertial sensor. The bicycle model is used in order to compute the coordinates of the borders of the warning area in the "top-view" $(0, X, Y)$ coordinate system. The left and right borders of this warning area are computed using an iterative process, from the closest to the furthest point. Let L denote the width of the vehicle, N the number of points on one border, and $dt = \frac{1}{N}$ the time increment. θ, X_{center} and Y_{center} are initialized to 0 and updated at each iteration, and the coordinate (X_{b_l}, Y_{b_l}), (X_{b_r}, Y_{b_r}) of the next $\{$*left, right*$\}$ border points are computed as follows:

$$\begin{cases} \theta \leftarrow \theta + \psi dt \\ X_{center} \leftarrow X_{center} + V\cos\theta dt \\ Y_{center} \leftarrow Y_{center} + V\sin\theta dt \end{cases} \quad (1)$$

$$\begin{cases} X_{b_l} = X_{center} - \frac{L}{2}\sin\theta \\ Y_{b_l} = Y_{center} + \frac{L}{2}\cos\theta \end{cases} \quad (2)$$

$$\begin{cases} X_{b_r} = X_{center} + \frac{L}{2}\sin\theta \\ Y_{b_r} = Y_{center} - \frac{L}{2}\cos\theta \end{cases} \quad (3)$$

where b_l stands for *left border* and b_r stands for *right border*.

Figure 8 presents two examples of the warning area projected onto the image. On Fig. 8 (a), the vehicle is on a curve and follows the road. In this case, the warning area is located on the vehicle lane. On Fig. 8 (b), the vehicle is on a straight line but is turning to the left. In this case, the waning area is not located on the vehicle lane. However, in both cases, the warning area corresponds to the path the vehicle is going to. As a matter of fact, this area is well adapted to the collision mitigation system. Indeed the system must detect the obstacles that the vehicle is likely to collide with, that are not necessary located on the vehicle lane, but on the vehicle path. Moreover, the warning area is generated dynamically. No assumption about the movement of the obstacles is made, and so avoidance maneuvers can be addressed by the system (see scenarios 10 and 11 in section III).

One can notice the width of the warning area is set to L in the system, where L is the width of the vehicle. This ensures all the obstacles potentially colliding with the vehicle path will be taken into account: the detection rate will be maximal. However, because of some inaccuracies that could occur at various levels in the system (estimations of obstacle position, orientation, width, ego vehicle speed, etc), setting the width of the warning area to L could result in some false alarms. In order to reduce as much as possible the false alarm rate, one could choose to set the width of the warning area at a lower value, for example $\frac{2L}{3}$. The sensibility of the performances regarding the value of the width of the warning area will be tackled in future works.

[Figure 8 about here.]

C. Decision unit

The decision unit send a warning message to the automatic braking system if the three following conditions are fulfilled for a track:

- the certainty of the track after the fusion step is above 0.7,
- $0 <$ TTC ≤ 1 s,
- the intersection between the track and the warning area is not empty.

It should be noted that we do not assume at any time that the equipped vehicle stays on target: as soon as the target is no longer in the warning area, it is no longer taken into account (negative tests stress this important point in section III, especially in scenarios 10 and 11).

D. Automatic braking system

An additional brake circuit has been installed on the prototype vehicle along with an electric pump, a brake pressure sensor, and a electromagnetic sluice gate. The chosen strategy consists in decreasing as much as possible

the velocity of the vehicle before the collision. Thus, when a warning message is received, a pressure command of 90 bars is applied on the brakes -90 bars corresponds to the maximal pressure the system can handle. The prototype vehicle is equipped with ABS brake system so that the braking is as efficient as possible. Figure 9 shows the behavior of the system during a typical emergency braking: the trigger (reception of warning message), the pressure curve, the deceleration, and the velocity of the ego vehicle are measured over time. The pressure begins to increase $120\ ms$ after the reception of the warning message and reaches its maximum about $300\ ms$ later. During the first second, the average deceleration is about $-6\ m/s^2$ and the velocity is reduced by $6\ m/s$. Then the average deceleration is about $-8\ m/s^2$, and the velocity is reduced by $4\ m/s$ within the next $0.5\ s$. When an emergency braking is performed on a motionless obstacle (e.g. TTC $= 1\ s$ if no braking is applied), the process lasts for about $1.5\ s$ and the velocity is reduced by $10\ m/s$ before the collision. The kinetic energy is reduced by $10\ m\ (V-5)\ J$ where V is the velocity of approach of the vehicle and m its weight. For instance, with V = 14 m/s and m = 1500 kg, the kinetic energy is reduced by 135 kJ = 0.49 kWh before collision.

[Figure 9 about here.]

One should notice that once launched (when the TTC equals 1 second), the braking actually lasts for more than 1 second before the collision occurs. Indeed the velocity of the vehicle decreases as soon as the braking is engaged. As a matter of fact, the TTC decreases more slowly to 0 second than it would have without braking, and the dissipated kinetic energy is higher than the one would have been dissipated during a 1 second braking.

III. System assessment

Before presenting the results of the tests, we introduce the main features of the prototype vehicle and describe the sensors configuration process.

A. Features of the prototype vehicle

Figure 10 shows a photo of the prototype vehicle which is a Renault Scenic^{TM}. It is equipped with a stereoscopic sensor, a laser scanner, an automating braking system and two PC computers.

The stereo sensor has the following features. The used CCD cameras are $Sony^{TM}$ 8500 C with $Computar^{TM}$ Auto Iris $8.5\ mm$ focal length. The resolution of each image is 380 x 288 pixels. The images are 8 bits grey-scale. They are grabbed using a $Matrox^{TM}$ Meteor II card. The baseline is $b = 1\ m$, the height $h = 1.4\ m$ and the pitch $\theta = 8.5\ ^o$ in the resting position. Images are rectified on-line thanks to an homography matrix computed during the sensor configuration (see section III B), using bicubic interpolation. The frame rate is 25 Hz.
The used laser scanner is a $Sick^{TM}$ laser scanner. Its pitch is $\theta_l = 0\ ^o$, its height $h_l = 0.42$ m, and its offset $X_l = -0.50\ m$ in the "top-view" coordinate system (see Figure 7). The raw output of the laser scanner is a set of 200 laser points, positioned every $0.5\ ^o$ from $-50\ ^o$ to $50\ ^o$ with respect to the longitudinal axis of the vehicle. The frame rate is 38 *Hz*.

With these sensors, the range of the system is [0;36] m which allow the system to work up to an ego speed of 36 *m / s*.

A bi-Xeon running at 2.6 GHz is used for the perception task.

An additional computer is used for the activator control. Both computers are linked through a 100 Mb/s ethernet connection. Warning messages from the computer dedicated to the perception task are sent to the computer dedicated to the activator control through this connection.

[Figure 10 about here.]

B. Sensor configuration

Two configurations must been performed. The first one consists in the configuration of the stereo sensor in order to obtain a rectified epipolar geometry. This configuration is done through the process described in [19]. Homography matrix are obtained for left and right images. Images are then corrected online using bicubic interpolation. Figure 11 presents the used mire.

[Figure 11 about here.]

The second configuration consists in estimating the laser scanner pose with respect to the stereovision sensor. The relative position of the laser scanner is manually measured once the laser scanner is mounted on the vehicle. The laser scanner is adjusted so that its relative roll and yaw are negligible. Figure 12 shows the protocol used to estimate its pitch: an oblique plane (height H, length d_0) is placed at a distance d_1 in front of the laser scanner. The distance D measured by the laser scanner allows to compute the pitch θ_l as follows (under the little angles assumption): $\theta_l = \frac{H(d_0+d_1-D)}{Dd_0}$.

[Figure 12 about here.]

C. Quantitative tests

1) Criteria of efficiency:

In order to assess the efficiency of the system, we define several criteria used in the test scenarios:

- a track is $confirmed$ if the certainty about its existence after data fusion is above $S_0 = 0.7$, and if the intersection between the track and the warning area is not empty,
- an obstacle is $confirmed$ if the track is $confirmed$ and if $TTC_{Nom} < TTC \leq TTC_{Max}$,
- an obstacle is $confirmed\ late$ if the track is $confirmed$ and if $TTC_{Min} <$ TTC $\leq TTC_{Nom}$,
- an obstacle is $not\ confirmed$ if {the track is $confirmed$ and TTC $\leq TTC_{Min}$}, or if {the track is not $confirmed$}.

For the test scenarios, the following values are used:

$$\begin{cases} TTC_{Max} = 1.1s \\ TTC_{Nom} = 0.9s \\ TTC_{Min} = 0.5s \end{cases} \quad (4)$$

All the $confirmed$ obstacles which do not fulfill at least one of the following criteria are considered as $false\ alarms$:

- the obstacle is in the warning area,
- the height of the obstacle is above $0.4\ m$.

If road furniture (sign, barrier, tree, object along the road) or the road itself is $confirmed$ as an obstacle, this is considered as a $false\ alarm$.

2) Experimental protocol:

Figure 13 presents a typical HMI output. In this case an automatic emergency braking has been launched in front of a pedestrian. The pedestrian has been detected and is located in the warning area and its TTC is 0.98 second. The vehicle on the left has also been detected but it is not located on the warning area and its TTC is above 1 second, so the system would not have launched any emergency braking if this vehicle would have been the only obstacle in the scene.

The test scenarios are shown on Figures 14 to 24. All these scenarios were defined within the functional analysis of the ARCOS project. On each Figure, a diagram explains the situation, two photos illustrate the test, and tables of results are given for positive tests. On the diagrams, a cross indicates an obstacle where an emergency braking must be performed by the system. Each test is carried out 10 times. The tables of results indicate the distance of the obstacles, the velocity of the vehicle and the TTC when the emergency braking is launched, wether the track is $confirmed$ and wether a false alarm occurred. For negative test, we indicate only how many false alarms were observed.

In the different scenarios, we use a $1.8\ m$ high and $0.5\ m$ broad pedestrian, a 0.5 x 0.7 x $0.6\ m$ box, $2.3\ m$ x $1.5\ m$ x $4.5\ m$ vehicles, and a $1.6\ m$ high and $0.5\ m$ broad cyclist.
The velocity of the prototype vehicle is between 6 and $11\ m/s$ and is indicated on the diagram. The tests have been carried out by day time. The weather was partially cloudy.

[Figure 13 about here.]

3) Positive test scenarios:

Tests n^o 1 and 2 are intended for evaluating the capacity of the system to react when a motionless obstacle is in the lane of the vehicle, as well as assessing if objects located along the lane could generate false alarms. Tests n^o 1 and 2 have been carried out on both straight line and curve with curvature $c = 40\ m$. A detection failure occurred

in test $2-6$ (on straight line): a dazzling effect due to sun prevent the stereovision algorithm from detecting the pedestrian, so that the certainty of the track was no high enough.

Tests n^o 3, 4 and 5 are intended for evaluating the capacity of the whole system (obstacle detection and confirmation, and emergency braking) to be reactive when an obstacle appears suddenly in front of the vehicle. The obstacle is moving in tests n^o 3 and 4. For the test n^o 3, a catapult is used to propel a pedestrian on the lane at $2\ m/s$. It is launched so that the pedestrian arrives at the middle on the lane when the vehicle is located at $11\ m$ from the obstacle.

Tests n^o 6 and 7 are intended for evaluating the capacity of the system to be reactive when an obstacle appears suddenly after a tight curve, and how relevant is the use of the warning area. Tests n^o 6 and 7 correspond to dangerous urban situations. Tests n^o 3, 4, 5, 6 and 7 have been carried out on a straight line. For some tests, the tracks are $confirmed\ late$: this is either the result of an inaccuracy concerning the warning area, because of the noise of the inertial sensor, or the consequence of the limited field of view of cameras, especially for scenarios 6 and 7.

[Figure 14 about here.]

[Figure 15 about here.]

[Figure 16 about here.]

[Figure 17 about here.]

[Figure 18 about here.]

[Figure 19 about here.]

[Figure 20 about here.]

4) Negative test scenarios:

Tests n^o 8, 9, 10 and 11 are intended for evaluating the capacity of the system for managing vehicle following and avoidance without generating false alarms, and for assessing how relevant is the use of the warning area. Tests n^o 8, 9 and 10 have been carried out on both straight line and curve with curvature $c = 40\ m$. Test n^o 11 has been carried out on a straight line. One false alarm occurred in scenario 9 and is the result of an uncorrect matching during the association task. The followed vehicle was matched with the static vehicle along the lane so that the estimated relative velocity was incorrect.

[Figure 21 about here.]

[Figure 22 about here.]

[Figure 23 about here.]

[Figure 24 about here.]

5) Results:

For the 90 positive tests and 70 negative tests carried out:

- the $obstacle\ detection\ rate$ is $(90-8)/90$ = **91.11%**,
- the $late\ obstacle\ detection\ rate$ is $7/90$ = **7.71%**,
- the $non\ detection\ rate$ is $1/90$ = **1.12%**,
- the $false\ alarm\ rate$ is $1/160$ = **0.63%**.

D. Qualitative tests

In order to have a more precise idea about the false alarm rate, qualitative tests have been carried out on different road types : freeway, highways, rural roads and downtown. All these tests took place on the French road network around Paris.

1) Experimental protocol: These tests have been carried out in real driving situations. The automatic braking system was turned off and only the warning messages were checked. In normal driving situations, an automatic system should never be launched. Each time an emergency braking would have been launched is thus considered as a false alarm.

The tests have been carried out under various meteorological situations: sunny, cloudy, rainy, and under various traffic situations: low traffic to dense traffic.

2) Tests on freeways: $403\ km$ have been ridden on freeways. The velocity was up to $36\ m\ /\ s$. No false alarm was observed during these tests.

Figure 25 (a) and (b) presents some typical freeway situations under which the system has been tested.

3) Tests on highways and rural roads: $78\ km$ have been ridden on highways and $116\ km$ on rural roads. The velocity was up to $25\ m\ /\ s$. No false alarm was observed during these tests.

Figure 25 (c) (d) presents some typical highway situations, and Figure 25 (e) (f) some rural road situations under which the system has been tested.

[Figure 25 about here.]

4) Tests in downtown: The downtown tests are certainly the most challenging tests since the context is the more complex. $140\ km$ have been ridden in downtown and in urban areas. The velocity was up to $14\ m/s$. A false alarm was observed twice. The first one is due to a matching error during association, and the second one is due to a false target detected by stereovision on a uphill gradient portion.

Figure 26 presents some typical urban situations under which the system has been tested.

[Figure 26 about here.]

5) Qualitative tests results overview: For the 737 km ridden, two false alarms were observed. The false alarm rate is thus 2.7 false alarms for 1000 km. No false alarm was observed either on freeways or on highways and rural roads. The two remaining false alarms were observed in downtown. Thus, the false alarm rate in downtown is thus 1.4 false alarm for 100 km.

These results are quite promising, even if the false alarm rate must be reduced by a factor of about 1000 before the system can be envisaged to be put in the hands of common driver.

IV. Remaining issues: how to tackle them ?

This study can be seen as a performance report about the version 1.0 of the collision mitigation system RESCUE. The following conclusions are the results of the analysis of the tests carried out.

Concerning the detection rate, the remaining non detections are due to a technological issue of the used CCD cameras. Their dynamic range is not high enough to handle all the driving situations one can meet. As a matter of fact, using cameras with higher dynamic range, such as CMOS cameras, could improve this point.

Concerning the remaining false alarms, the first issue concerns the matching process, between tracks and targets which could be improved as described in [20]. The second issue is about stereovision. One way to tackle this problem could be to implement a second stereovision process to confirm the existence of obstacles detected initially. Basically, an additional stereovision algorithm directly launched in the part of the image corresponding to a detected obstacle could evaluate a criteria so as to confirm the existence of the obstacle.

The system has proven to be reactive, while some improvements can be made. Some detections were late. These delays mainly occurred in situations were the field of view of the cameras was too small. As a matter of fact, the base of the stereo sensor should be reduced, in order to handle better near obstacles appearing suddenly. The resolution of the cameras should be increased at the same time to be able to detect further obstacles. A crucial point for the reactivity of the system is the time of convergence of the process leading to the estimation of the relative speed of obstacles. This point could be improved. Indeed, a method for fast Kalman convergence with various initial conditions has been proposed in [21] and could be used in our system.

Beyond this algorithmic considerations, our experiments gave us some feelings about features the sensors should meet to handle the different situations with good reactivity. First, the sensors should process data at a relatively high frequency. Second, the position of the sensors should be chosen carefully. Concerning our system, best results were obtain when:

- the frequency of the slowest sensor (i.e. the CCD camera) is 25 Hz,
- the laser scanner height and pitch are adjusted to detect obstacles from 0.40 up to 1.5 meters high in the whole range of the system (basically $0 - 36\ m$),
- the field of view of the stereo sensor is included into the field of view of the laser scanner.

In future works, we will take into account the speed of the equipped vehicle to launch the emergency braking. The constant TTC criteria (emergency braking launched when TTC equals 1 second) seems indeed not accurate enough for full efficiency, above all at low speed: the emergency braking should be launched only at the time required for stopping before the collision, that can be under 1 second when the speed is low (basically under *10 m / s*).

Eventually, the auto-calibration of the set of sensors (stereovision and stereovision with respect to laser scanner) is an essential task for the viability of such a system in the automotive context. This task is being investigated at the moment.

V. Conclusion

In this paper, the version 1.0 of the RESCUE (REduce Speed of Collision Under Emergency) collision mitigation system was proposed and evaluated. The obstacles detection process, based on the algorithm presented in [14], was improved. An efficient way to predict the vehicle path as well as the automatic braking system was detailed. Then typical test scenarios were introduced. 90 positive tests and 70 negative tests were performed. All these tests were demonstrated in real time at the final ARCOS symposium. Concerning these tests, the false alarm rate is 0.63% and the detection rate is 98.82%. The RESCUE system has proved to be reactive in special urban scenarios, including crossroads scenarios. $737\ km$ have also been ridden in countryside, on rural roads, freeways and highways. Concerning these tests, the false alarms rate is 2.7 false alarms every $1000\ km$ ridden (the remaining false alarms were observed in downtown, no false alarm occurred in rural roads, highways or freeways). These experiments show the RESCUE system is quite promising, even if the false alarm rate must be reduced by a factor of about 1000 before the system can be put in the hands of common driver. In the next versions of the RESCUE system, the remaining false alarms problem will be addressed and we will investigate how the system could be extended to be used in other applications such as Stop'n'Go and ACC.

Acknowledgments

This research is partly funded by the ARCOS project. The authors would like to thank the LROP unit and especially Dominique Guichon, Christian Le Verger, Didier Dominois as well as Jean Marie Chevreau for their helpful assistance.

REFERENCES

[1] Observatoire National Interministriel de Scurit Routire, La scurit routire en France, bilan annuel 2001, DSCR, 2002.

[2] eSafety Working Group on Road Safety, "eSafety Final Report of the eSafety Working Group on Road Safety", November 2002, $http://ivsource.net/public/030104_eSafetyFinalReport.pdf$

[3] Cheok K. C., Smid G. E., McCune D.J., A Multisensor-Based Collision Avoidance System with Application to a Military HMMWV, Proceedings of IEEE Intelligent Transportation Systems Conference, 2000.

[4] Gavrila M., Kunert M., Lages U., "A Multi-Sensor Approach for the Protection of Vulnerable Traffic Participants the PROTECTOR Project", Proceedings of IEEE Instrumentation and Measurement Technology Conference, Budapest, Hongrie, 21-23 mai, 2001.

[5] Meinecke MM., Obojski M., Tns M., Doerfler R., Marchal P., Letellier L., Gavrila D., Morris R., "Approach for Protection of Vulnerable Road Users using Sensor Fusion Techniques", Proceedings of International Radar Symposium, Dresden, Germany, Sept 30 Oct 2, 2003.

[6] Blosseville J.M., "Some Achievements of ARCOS on Driver Assistance Functions", Proceedings of 5th European Congress and Exhibition on Intelligent Transport Systems, Hannover, Germany, Germany, 1-3 June 2005.

[7] Bertozzi M., Broggi A., "GOLD: A Parallel Real-Time Stereo Vision System for Generic Obstacle and Lane Detection", IEEE Transactions on Image Processing, Vol. 7, N1, January 1998.

[8] Mendes A., Conde Bento L., Nunes U., "Multi-target Detection and Tracking with a Laserscanner", Proceedings of IEEE Intelligent Vehicles Symposium 2004, pp 796-801, Parma, Italy, June 14-17, 2004.

[9] Sugimoto S., Tateda H., Takahashi H., Okutomi M., "Obstacle Detection Using Millimeter-Wave Radar and Its Visualization on Image Sequence", Proceedings of International Conference on Pattern Recognition 2004, Cambridge, UK, August 23 - 26, 2004.

[10] Langheim J., Buchanan A., Lages U., Wahl, "CARSENSE: New Environment Sensing for Advanced Driver Assistance Systems", Proceedings of IEEE Intelligent Vehicles Symposium 2001, National Institute of Informatics, Tokyo, Japan, June 3-6, 2001.

[11] Mobus R., Kolbe U., "Multi-Target Multi-Object Tracking, Sensor Fusion of Radar and Infrared", Proceedings of IEEE Intelligent Vehicle Symposium 2004, pp 732-737, Parma, Italy, June 14-17, 2004.

[12] Steux B., "Fade: A Vehicle Detection and Tracking System Featuring Monocular Color Vision and Radar Data Fusion", Proceedings of IEEE Intelligent Vehicles Symposium 2002, Versailles, France, June 18 - 20, 2002.

[13] Stiller C., Hipp J., Rssig C., Ewald A., "Multisensor Obstacle Detection and Tracking", Proceedings of the IEEE Intelligent Vehicles Symposium 1998, Stuttgart, Germany, October 28-30, 1998.

[14] Labayrade R., Royere C., Gruyer D., Aubert D., "Cooperative Fusion for Multi-Obstacles Detection with Use of Stereovision and Laser Scanner", Proceedings of IEEE International Conference of Autonomous Robots 2003, Coimbra, Portugal, June 30 - July 3, 2003.

[15] Labayrade R., Aubert D., Tarel J. P., "Real Time Obstacle Detection on Non Flat Road Geometry through V-Disparity Representation", IEEE Intelligent Vehicles 2002, Versailles, France, June 18 - 20, 2002.

[16] Labayrade R., Aubert D., "Robust and Fast Stereovision Based Obstacles Detection for Driving Safety Assistance", IEICE Trans. Inf. Syst., pp 80-88, Vol. E87-D, No.1, January 2004.

[17] Shafer G., "A Mathematical Theory of Evidence", Princeton University Press, 1976.

[18] Gruyer D., Royere C., Labayrade R., Aubert D., "Credibilistic Multi-Sensor Fusion for Real Time Embedded Application. Applied to the Near Obstacle Detection and Tracking", Proceedings of IEEE International Conference of Autonomous Robots 2003, Coimbra, Portugal, June 30 - July 3, 2003.

[19] Zhang Z., Deriche R., Luong Q.-T., Faugeras O., "A Robust Approach to Image Matching: Recovery of the Epipolar Geometry", Proceedings of Int'l Symposium of Young Investigators on Information-Computer-Control, pp 7-28, Beijing, China, February 1994.

[20] Kaempchen N., Buehler M., Dietmayer K., "Feature-Level Fusion for Free-Form Object Tracking using Laserscanner and Video", Proceedings of IEEE Intelligent Vehicles Symposium 2005, pp 453-458, Las Vegas, USA, June 6-8 2005.

[21] Franke U., Rabe C., "Kalman Filter based Depth from Motion with Fast Convergence", Proceedings of IEEE Intelligent Vehicles Symposium 2005, pp 181-186, Las Vegas, USA, June 6-8 2005.

LIST OF FIGURES

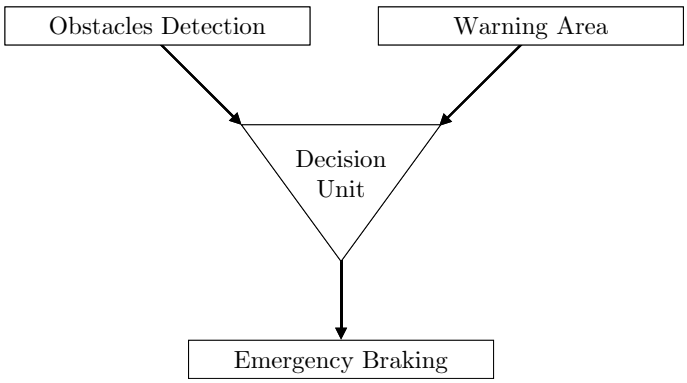

Fig. 1. System overview.

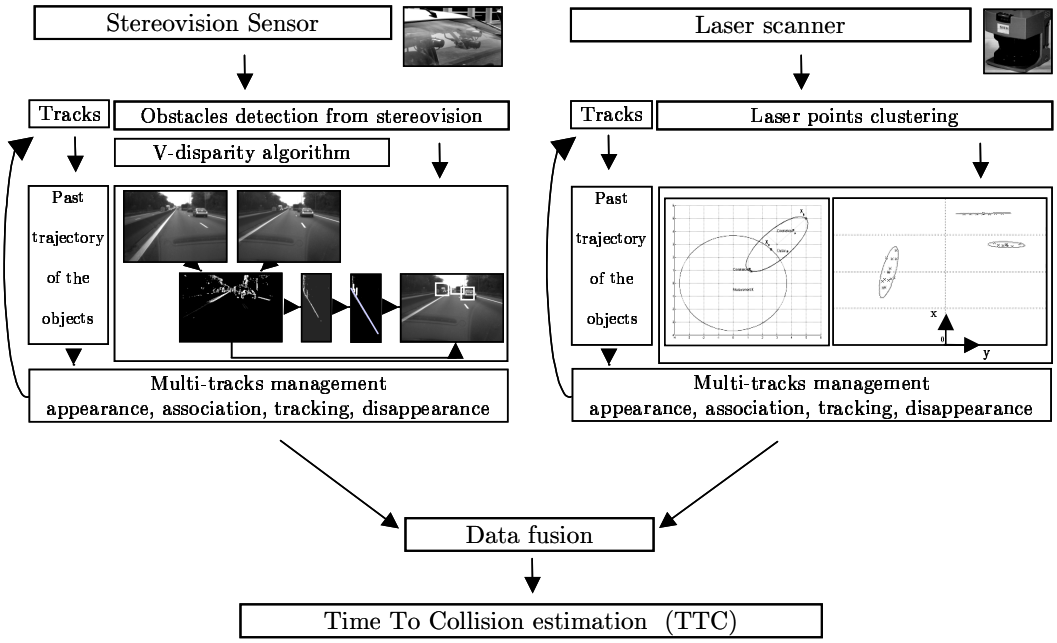

Fig. 2. Obstacles detection system overview.

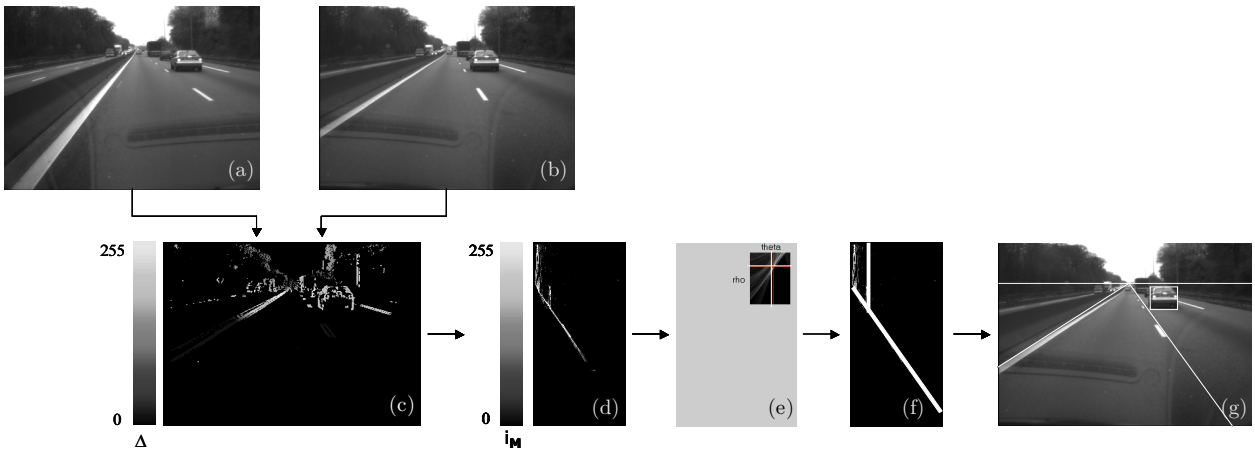

Fig. 3. V-disparity process overview. See text for details.

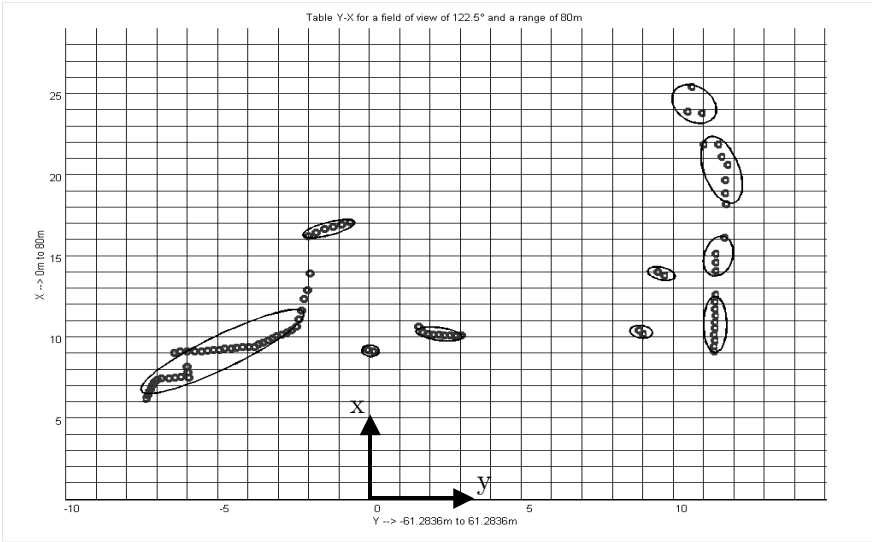

Fig. 4. Example of dynamic clustering (black ellipsoids) from laser scanner raw data (little circles).

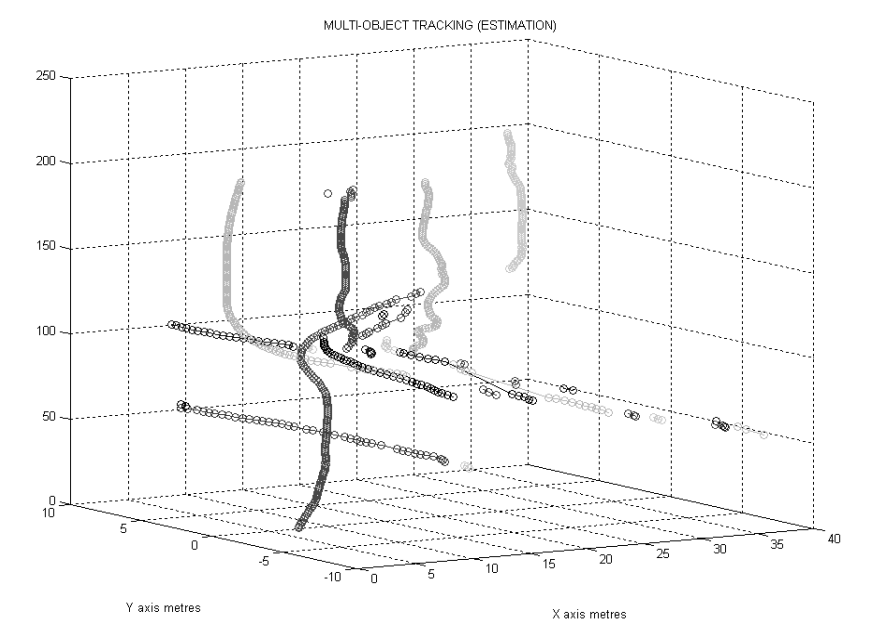

Fig. 5. Result of tracking of multi-objects over time. The vertical axis represents the number of steps of time (one step of time lasts for 26 ms).

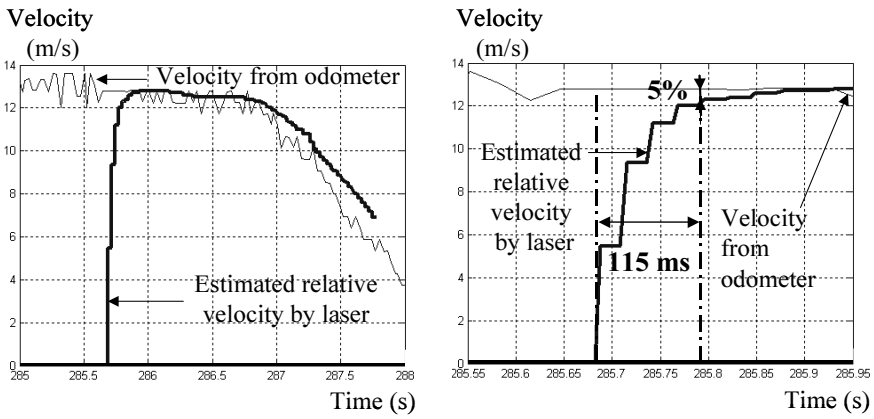

Fig. 6. Relative velocity estimated from the laser scanner data.

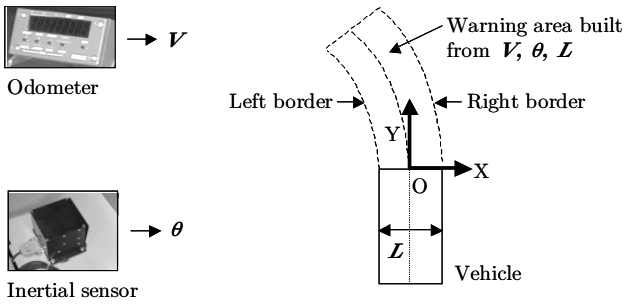

Fig. 7. Warning area in the top-view coordinate system.

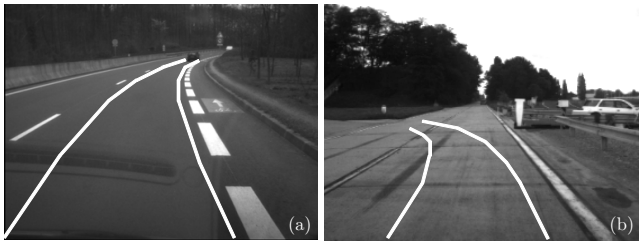

Fig. 8. Examples of warning areas projected onto the image. See text for details.

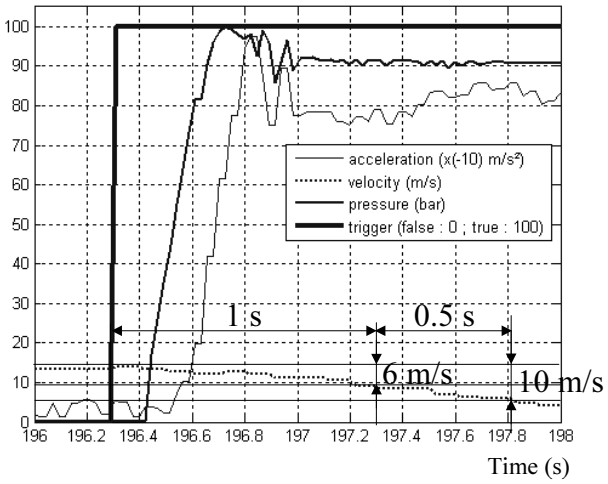

Fig. 9. Pressure, acceleration and velocity during emergency braking.

Fig. 10. The prototype vehicle, equipped with stereovision sensor, laser scanner sensor, odometer, inertial sensor, and automatic braking system.

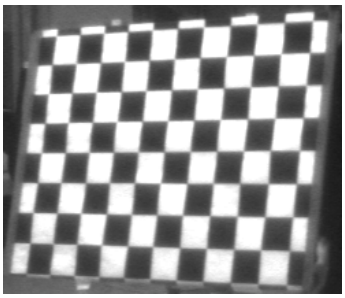

Fig. 11. Typical image of the mire used for the stereo sensor configuration.

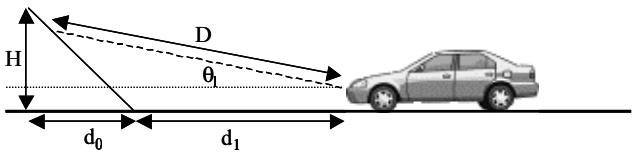

Fig. 12. Laser scanner configuration protocol.

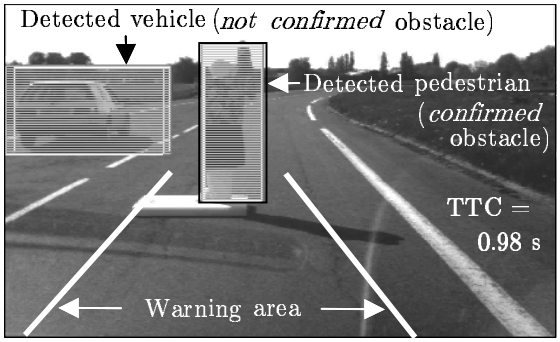

Fig. 13. Typical Human Machine Interface of the collision mitigation system.

Test N°	Distance (m)	Velocity (m/s)	TTC (s)	Track confirmation	False Alarm	Test N°	Distance (m)	Velocity (m/s)	TTC (s)	Track confirmation	False Alarm
1-1 (SL)	8.83	9.36	0.94	Yes	No	1'-1 (C)	10.87	11.05	0.98	Yes	No
1-2 (SL)	9.73	9.57	0.98	Yes	No	1'-2 (C)	10.42	11.24	0.93	Yes	No
1-3 (SL)	9.49	10.05	0.94	Yes	No	1'-3 (C)	10.11	10.87	0.93	Yes	No
1-4 (SL)	9.20	9.06	1.00	Yes	No	1'-4 (C)	10.47	11.08	0.94	Yes	No
1-5 (SL)	10.20	10.19	0.95	Yes	No	1'-5 (C)	10.04	10.74	0.93	Yes	No
1-6 (SL)	10.64	10.99	0.97	Yes	No	1'-6 (C)	10.79	10.97	0.98	Yes	No
1-7 (SL)	9.67	10.03	0.96	Yes	No	1'-7 (C)	10.63	11.10	0.96	Yes	No
1-8 (SL)	10.00	10.30	0.97	Yes	No	1'-8 (C)	10.01	10.36	0.97	Yes	No
1-9 (SL)	9.89	9.95	1.01	Yes	No	1'-9 (C)	9.85	10.47	0.94	Yes	No
1-10 (SL)	8.00	8.46	0.95	Yes	No	1'-10 (C)	10.09	10.31	0.98	Yes	No

Fig. 14. Scenario 1 (SL: on Straight Line - C: in Curve) - Emergency braking on a pedestrian.

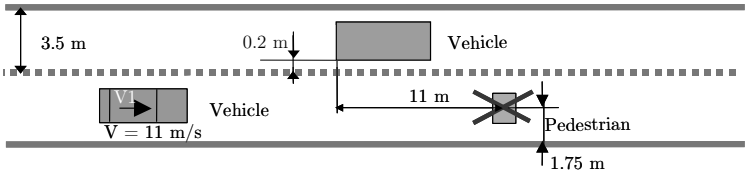

Test N°	Distance (m)	Velocity (m/s)	TTC (s)	Track Confirmation	False Alarm
2-1 (SL)	10.55	10.64	0.99	Yes	No
2-2 (SL)	9.60	9.80	0.98	Yes	No
2-3 (SL)	9.94	10.11	0.98	Yes	No
2-4 (SL)	9.86	10.10	0.98	Yes	No
2-5 (SL)	9.81	10.57	0.93	Yes	No
2-6 (SL)	-	-	-	No	No
2-7 (SL)	9.69	9.83	0.99	Yes	No
2-8 (SL)	9.54	9.74	0.97	Yes	No
2-9 (SL)	10.28	10.45	0.98	Yes	No
2-10 (SL)	10.45	10.60	0.99	Yes	No

Test N°	Distance (m)	Velocity (m/s)	TTC (s)	Track Confirmation	False Alarm
2'-1 (C)	10.45	11.08	0.94	Yes	No
2'-2 (C)	10.84	11.35	0.96	Yes	No
2'-3 (C)	10.43	11.24	0.93	Yes	No
2'-4 (C)	9.76	10.71	0.91	Yes	No
2'-5 (C)	9.94	10.62	0.94	Yes	No
2'-6 (C)	10.28	11.07	0.93	Yes	No
2'-7 (C)	9.49	10.17	0.93	Yes	No
2'-8 (C)	10.29	10.96	0.94	Yes	No
2'-9 (C)	10.81	11.19	0.97	Yes	No
2'-10 (C)	9.72	10.48	0.93	Yes	No

Fig. 15. Scenario 2 (SL: on Straight Line - C: in Curve) - Emergency braking on a pedestrian with vehicle on the side.

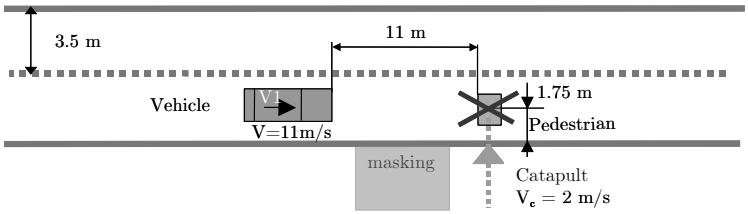

Test N°	Distance (m)	Velocity (m/s)	TTC (s)	Track Confirmation	False Alarm
3-1	11.26	12.26	0.95	Yes	No
3-2	10.80	11.40	0.95	Yes	No
3-3	11.86	12.80	0.95	Yes	No
3-4	8.80	11.20	0.79	Yes - Late	No
3-5	10.90	11.26	0.97	Yes	No
3-6	9.70	10.08	0.96	Yes	No
3-7	10.18	10.54	0.97	Yes	No
3-8	10.31	10.96	0.94	Yes	No
3-9	10.64	10.83	0.98	Yes	No
3-10	10.43	10.67	0.98	Yes	No

Fig. 16. Scenario 3 - Emergency braking on a pedestrian appearing suddenly from the side.

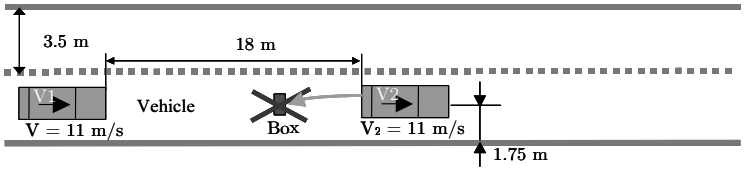

Test N°	Distance (m)	Velocity (m/s)	TTC (s)	Track Confirmation	False Alarm
4-1	11.06	11.24	0.98	Yes	No
4-2	11.08	11.80	0.94	Yes	No
4-3	11.74	11.87	0.99	Yes	No
4-4	10.85	10.99	0.99	Yes	No
4-5	10.45	11.05	0.94	Yes	No
4-6	9.88	10.11	0.98	Yes	No
4-7	10.95	11.42	0.96	Yes	No
4-8	9.74	11.49	0.85	Yes - Late	No
4-9	10.69	10.93	0.98	Yes	No
4-10	11.12	11.39	0.98	Yes	No

Fig. 17. Scenario 4 - Emergency braking on a box thrown from a followed vehicle.

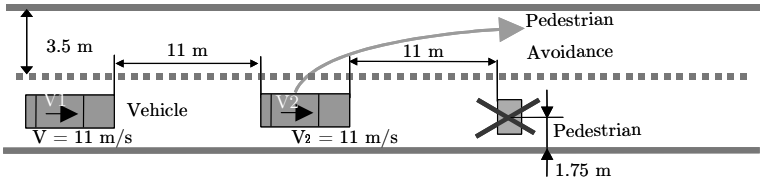

Test N°	Distance (m)	Velocity (m/s)	TTC (s)	Track Confirmation	False Alarm
5-1	8.43	9.16	0.93	Yes	No
5-2	9.08	9.27	0.98	Yes	No
5-3	8.99	9.73	0.94	Yes	No
5-4	8.87	9.69	0.92	Yes	No
5-5	9.92	10.16	0.98	Yes	No
5-6	9.97	10.22	0.98	Yes	No
5-7	9.44	9.99	0.95	Yes	No
5-8	7.87	9.73	0.81	Yes - Late	No
5-9	8.58	8.64	0.99	Yes	No
5-10	9.39	9.81	0.96	Yes	No

Fig. 18. Scenario 5 - Vehicle following and emergency braking on a pedestrian appearing suddenly.

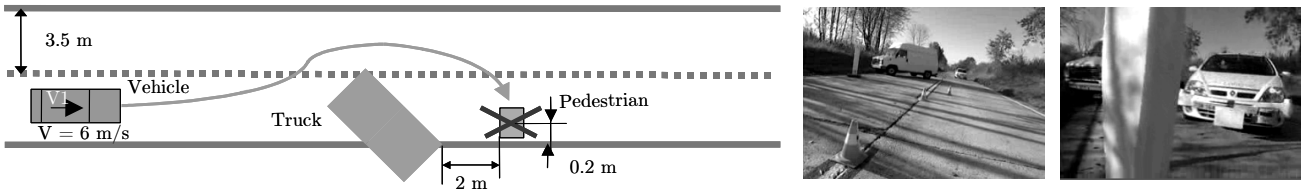

Test N°	Distance (m)	Velocity (m/s)	TTC (s)	Track Confirmation	False Alarm
6-1	5.43	5.84	0.93	Yes	No
6-2	5.99	6.22	0.96	Yes	No
6-3	5.47	5.74	0.95	Yes	No
6-4	5.98	6.28	0.95	Yes	No
6-5	5.32	5.86	0.91	Yes	No
6-6	5.44	6.08	0.89	Yes - Late	No
6-7	5.49	5.85	0.94	Yes	No
6-8	5.52	6.38	0.87	Yes - Late	No
6-9	5.78	5.88	0.98	Yes	No
6-10	5.21	5.54	0.94	Yes	No

Fig. 19. Scenario 6 - Emergency braking on a pedestrian hidden by a truck.

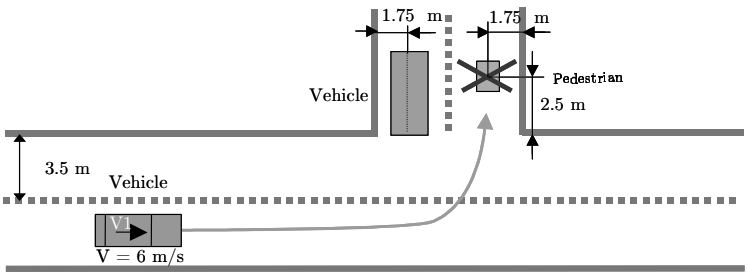

Test N°	Distance (m)	Velocity (m/s)	TTC (s)	Track Confirmation	False Alarm
7-1	5.94	5.97	0.99	Yes	No
7-2	5.21	5.36	0.97	Yes	No
7-3	5.44	6.11	0.89	Yes - Late	No
7-4	5.37	6.14	0.87	Yes - Late	No
7-5	5.62	5.82	0.97	Yes	No
7-6	5.84	5.94	0.98	Yes	No
7-7	5.23	5.63	0.93	Yes	No
7-8	5.87	5.97	0.98	Yes	No
7-9	5.95	6.04	0.99	Yes	No
7-10	5.32	5.91	0.9	Yes	No

Fig. 20. Scenario 7 - Emergency braking on a pedestrian located on a cross-road and hidden by a vehicle.

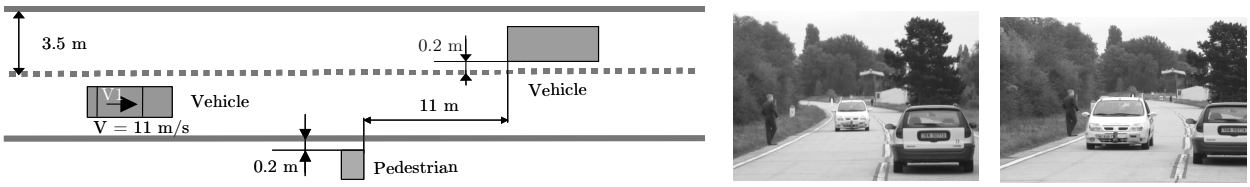

Fig. 21. Scenario 8 - Vehicle and pedestrian on the side. No false alarm occurred.

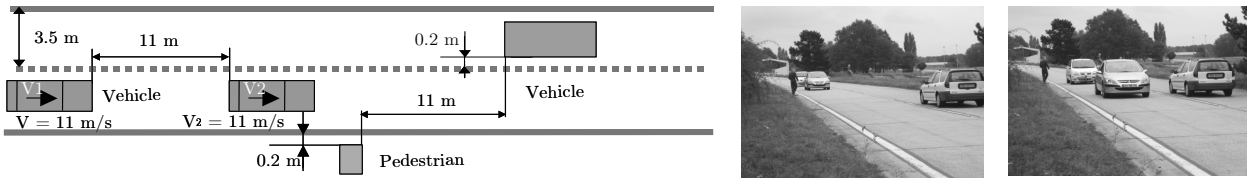

Fig. 22. Scenario 9 - Vehicle following with pedestrian and vehicle on the side. 1 false alarm occurred (test in curve).

Fig. 23. Scenario 10 - Cyclist following and avoidance. No false alarm occurred.

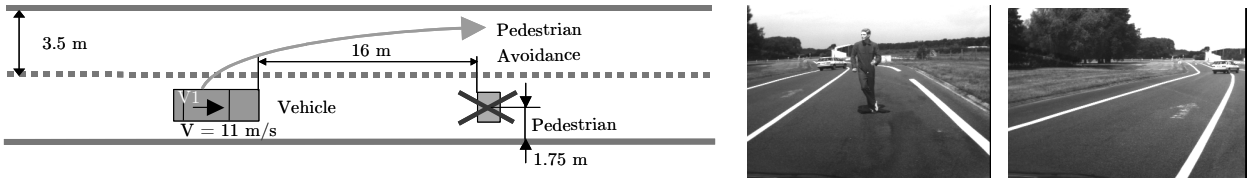

Fig. 24. Scenario 11 - Pedestrian avoidance. No false alarm occurred.

Fig. 25. Typical images of freeway and rural road situations. (a) truck following on a freeway, dense traffic - (b) freeway with low traffic - (c)(d) peri-urban highway - (e)(f) rural road with tight uphill gradient.

Fig. 26. Typical images of urban situations. (a) pedestrian crossing - (b) road works - (c) car driving out of parking lot - (d) car and bus traffic - (e) narrow road and tight curve - (f) tight curve, non flat road - (g) dense traffic - (h) road with high roll - (i) narrow paved road, tight curve.